OMTO, Volume *18*

Supplemental Information

Design of an Interferon-Resistant Oncolytic HSV-1 Incorporating Redundant Safety Modalities for Improved Tolerability

Edward M. Kennedy, Terry Farkaly, Peter Grzesik, Jennifer Lee, Agnieszka Denslow, Jacqueline Hewett, Jeffrey Bryant, Prajna Behara, Caitlin Goshert, Daniel Wambua, Ana De Almeida, Judith Jacques, Damian Deavall, James B. Rottman, Joseph C. Glorioso, Mitchell H. Finer, Brian B. Haines, Christophe Quéva, and Lorena Lerner

SUPPLEMENTAL INFORMATION

Design of an interferon-resistant oncolytic HSV-1 incorporating redundant safety modalities for improved tolerability

Edward M. Kennedy,[1]* Terry Farkaly,[1]* Peter Grzesik,[1] Jennifer Lee,[1] Agnieszka Denslow,[1] Jacqueline Hewett,[1] Jeffrey Bryant,[1] Prajna Behara,[1**] Caitlin Goshert,[1**] Daniel Wambua,[1] Ana de Almeida,[1] Judith Jacques,[1] Damian Deavall,[2] James B. Rottman,[3] Joseph C. Glorioso,[4] Mitchell H. Finer,[1**] Brian B. Haines,[1] Christophe Quéva,[1] Lorena Lerner[1]

[1]Oncorus, Inc., Cambridge, MA, USA; [2]ApconiX, Alderley Park, Mereside, Macclesfield, UK; [3]Athenaeum Pathology Consulting, LLC, Sudbury, MA, USA; [4]University of Pittsburgh, School of Medicine, Department of Microbiology and Molecular Genetics, Pittsburgh, PA, USA

METHODS

Total RNA Isolation from Cells in Culture

Media was aspirated, and cells from each well were collected in Trizol. 200µL chloroform was added to 1mL Qiazol Lysis Reagent and vortexed vigorously for 15 sec. After 2-min incubation at room temperature, samples were centrifuged at 12,000 x g for 15 minutes at 4℃. 0.5 mL isopropanol and 1 µL of glycoblue was added and vortexed briefly. Samples were incubated at room temperature for 10 min and centrifuged at 12,000 x g for 10 mins at 4℃. 1mL 75% ice-cold ethanol per and 1:10 3M sodium acetate were added to each sample, mixed gently and incubated on ice 2 min, then centrifuged at 7500 x g for 5 min at 4℃. 1mL 75% ice-cold ethanol per was added, samples were incubated on ice for 2 min, and centrifuged at 7500 x g for 5 min at 4℃. RNA pellet was dried and resuspended in 40 µL RNAse-free water.

nanoString TagSet Gene Expression

Gene expression using nanoString (NanoString Technologies Inc. Seattle, WA) was performed per the manufacturer protocol (PlexSet Reagents for Gene Expression User Manual). The raw data (.RCC files) quality control was conducted. Raw data was checked through the nSolver 4.0 software to ensure 1) binding density was appropriate, 2) ligation controls were in the appropriate range, and 3) positive hybridization controls were correct.

Datasets were normalized in nSolver™ 4.0 by background thresholding the geometric mean across the negative controls, any samples outside of the 0.3 to 3 normalization factor range were omitted. Subsequently, normalization of the geometric mean of the positive controls was conducted to account for hybridization efficiency. CodeSet content is normalized to the geometric mean across 3 housekeeping genes (ABCF1, GUSB, HPRT1). Any samples for which the normalization factors were outside of the 0.1 to 10 range were omitted.

A heat map summary of the miRNA ratios was generated using Broad Institute's Morpheus software https://software.broadinstitute.org/morpheus/.

Gene Expression by RT-qPCR

Isolated total RNA from cell cultures samples were normalized to 500 ng of input for reverse transcription using oligo(dT) primers and cDNA synthesis using SuperScript IV (ThermoFisher, 18090010) according to the manufacturer's protocol. Each cDNA sample (5 µL) was added to MicroAmp Optical 96-well reaction plates (Invitrogen, ThermoFisher Applied Biosystems™, N8010560) containing 15 mL of Taqman Fast Advanced Master Mix (Invitrogen, ThermoFisher Applied Biosystems, 4444554). RT-qPCR was performed on Applied Biosystems QuantStudio 5 thermocycler with 1 cycle of 95℃ for 20 sec, followed by 40 cycles of 95℃ for 1 sec denaturation and 60℃ for 20 sec (annealing/extension). Specific NFQ-MGB TaqMan Advanced assay probes (ThermoFIsher PN4331348) were used for each gene present in the assay. $2^{\Delta\Delta Ct}$ calculations were performed and results were reported as ratios by normalizing the target gene to a housekeeping mRNA (GAPDH, ThermoFisher PN4448489), and each target gene to each probe for both negative siRNA and target siRNA.

miRNA RT-qPCR

Isolated RNA tissue samples were normalized to 10 ng of input for reverse transcription and cDNA synthesis using Taqman Advanced miRNA cDNA Synthesis Kit (Invitrogen, ThermoFisher Applied Biosystems™, A28007) according to the manufacturer's protocol. Each cDNA sample (5 µL) was added to MicroAmp Optical 96-well reaction plates (Invitrogen, ThermoFisher Applied Biosystems™, N8010560) containing 15 µL of Taqman Fast Advanced Master Mix (Invitrogen, ThermoFisher Applied Biosystems, 4444554). RT-qPCR was performed on Applied Biosystems QuantStudio 5 thermocycler with 1 cycle of 95℃ for 20 sec, followed by 40 cycles of 95℃ for 1 sec denaturation and 60℃ for 20 sec (annealing/extension). Specific NFQ-MGB TaqMan Advanced miRNA assay probes (Invitrogen, ThermoFisher Applied Biosystems, A25576) were used for each miRNA present in the assay. A miRNA standard curve was established using a universal standard curve with a non-mammalian exogenous 5' phosphorylated standard, Arabidopsis thaliana miRNA ath-159a (Invitrogen, ThermoFisher, 478411_mir). miRNA copy numbers were calculated using the synthetic miR ath-159a, utilizing the similarity of short miRNA sequences to amplify at the same rate (within 0.5 cycle threshold) with no cross-specificity between synthetic and human miRNA. A dynamic range of 10,000,000 to 100 copies was established and verified with synthesized human miRNA standards to validate ath-159a as a universal miRNA standard curve. Final copy number per 10 ng RNA was quantified and normalized to determine fold change expression over the negative mimic control.

Mouse Tissue RNA Extraction

Whole brain mouse tissues were sourced from Brain Bits LLC (Springfield, IL). Samples were flash frozen immediately after resection from C57BL/6 mice. Additional tissue samples were obtained from Charles River Laboratories (Wilmington, MA). Twenty mg sections were cut by scalpel and placed in a 1.5 mL Eppendorf tube and stored at -80℃.

For RNA isolation, tissue samples were thawed on ice. Qiazol (Qiagen) and chloroform were chilled on ice prior to use. Qiazol (700 µL) was added to each tube containing a tissue section, and disposable RNase-free pestles were used to homogenize the tissue. Subsequently, 140 µL of chloroform was added and centrifuged at maximum speed for 10 min. The upper aqueous phase (300 µL) was transferred to a new tube and 450 µL of 100% ethanol at room temperature was then added and mixed. Approximately 700 µL of this mixture was transferred to a Qiagen miRneasy column. The remaining steps in this process was performed according to the manufacturer's protocol (Qiagen miRneasy Kit, 217004). Each RNA sample in this report was analyzed by a NanoDrop spectrophotometer (ThermoFisher Scientific, Wilmington, MA) to confirm sample quality as recommended by nCounter® miRNA Expression Assay User Manual.

nanoString Mouse miRNA Profiling

miRNA profiling using nanoString (NanoString Technologies Inc. Seattle, WA) was performed exactly as per the manufacturer protocol (nCounter® miRNA Expression Assay User Manual).

All individual tissue samples were analyzed with the mouse miRv1.5 panel on the nanoString Sprint instrument. Sample preparation was performed exactly per the manufacturer recommendations, and the raw data (.RCC files) quality control was conducted. Raw data was checked through the nSolver 4.0 software to ensure 1) binding density was appropriate, 2) ligation controls were in the appropriate range, and 3) positive hybridization controls were correct. These analyses were performed with nSolver™ 4.0 and exported raw data.

Datasets were normalized in nSolver™ by background thresholding the geometric mean across the negative controls, any samples outside of the 0.3 to 3 normalization factor range were omitted. Subsequently, normalization to the geometric mean of the positive controls was conducted to account for hybridization efficiency and was scaled to all endogenous and housekeeping genes to 1,000,000 total count of the lane. Any samples for which the normalization factors were outside of the 0.1 to 10 range were omitted.

A heat map summary of the miRNA ratios was generated using Broad Institute's https://software.broadinstitute.org/morpheus/ Morpheus software.

In silico generation of miR-T cassettes

A computer script written in the Python programming language was written to generate miR-T cassettes that are optimal for RISC targeting. This script inserts the correct target sequence in the cassette such that no two targets are repeated in-line, to prevent potential steric occlusion of RISC occupied adjacent targets. It also searches for tumor specific miRNA targets or seed targets that may be present by chance as random spacers are generated. If these sequences are encountered, these candidates are eliminated. Then an automated effort to eliminate structured elements is performed, as RNA secondary structure is also a known inhibitor of RISC targeting.[1] The optimal lowest predicted structured cassette is then selected. These cassettes were then validated individually with a well validated tool to objectively detect miRNA binding sites called miRANDA.[2]

Biodistribution Studies

BALB/c mice bearing established (~100 mm^3) dual flank A20 tumors were administered $3x10^5$-$3x10^6$ PFU, depending upon the study of ONCR-159 into the right flank tumor. Tissues (injected and contralateral tumors, liver, and blood) were harvested 4, 24, 48, 72, and 168 hours post dose. Genomic viral DNA from tumors and liver was quantified using the nanodrop and diluted to 25 ng/µl in nuclease free water. Blood samples were diluted to 10 ng/µl. Five µl/well of either the DNA sample (corresponding to 125 ng of DNA from tumors or 50 ng of DNA from blood) or the US6 plasmid standard was used in a qPCR reaction, performed in technical triplicates, to detect HSV-1 genomes on a Quantstudio5 qPCR instrument with the following thermal cycler conditions: Hold Stage: 95˚C for 1 second, PCR stage: 95°C for 1 second, followed by 60˚C for 30 seconds. The PCR stage was performed for 45 cycles. Plasmid standards were used to generate a standard curve with known amount of copies corresponding to a set of Ct values. Based on this standard curve, the amount of HSV genome copies in the sample were calculated.

The copy number calculations were done on the Quantstudio software. Since 125 ng/well of tumor DNA or 50 ng/well of blood DNA was loaded in the qPCR assay, a conversion factor was applied to the copy number in order to plot them as copies/µg of DNA. Technical duplicates were averaged and the results of individual animals within each group were plotted using GraphPad software. Conversion of copy number to copies/µg and calculations of averages were done on Microsoft Excel. PCR Primer/probe: Fwd: 5'-CCCGCTGGAACTACTATGACA-3'; Rev: 5'-GCATCAGGAACCCCAGGTT-3'; Probe: 5'-TTCAGCGCCGTCAGCGAGGA-3' with FAM as the reporter dye and MGB-NFQ as the quencher.

Total RNA Isolation from Cells in Culture

Media was aspirated, and cells from each well were collected in Trizol. 200 µL chloroform was added to 1 mL Qiazol Lysis Reagent and vortexed vigorously for 15 seconds. After 2-minute incubation at room temp, samples were centrifuged at 12,000 x g for 15 minutes at 4℃. 0.5 mL isopropanol and 1 µL of glycoblue was added and vortexed briefly. Samples were incubated at room temperature for 10 minutes and centrifuged at 12,000 x g for 10 minutes at 4℃. 1 mL 75% ice-cold ethanol per and 1:10 3M sodium acetate were added to each sample, mixed gently and incubated on ice 2 minutes, then centrifuged at 7500 x g for 5 minutes at 4℃. 1 mL 75% ice-cold ethanol per was added, incubated on ice for 2 minutes, and centrifuged at 7500 x g for 5 minutes at 4℃. RNA pellet was dried and resuspended in 40 µL RNAse-free water.

nanoString TagSet Gene Expression

Gene expression using nanoString (NanoString Technologies Inc. Seattle, WA) was performed exactly as per the manufacturer protocol (PlexSet Reagents for Gene Expression User Manual). Each total RNA from cell culture samples were analyzed in a separate multiplexed reaction. nCounter TagSet technology consists of specific reporter tags comprised of unique fluorescent barcodes linked to specific nucleotide Tags. A biotinylated universal capture tag hybridizes to a pair of target-specific oligonucleotide probes that hybridize directly to single-stranded RNA targets. The universal capture tag anchors each target to the surface of a streptavidin-coated lane, followed by 2 custom oligonucleotide probes specific to target nucleic acid sequences. Once these probes are bound to their target nucleic acid sequences, unique fluorescent barcodes hybridize to the 5' region of the probe and the universal capture probe to the 3' region of the target nucleic acid probes to form a Tag Complex. Reporter tags each have a unique 6 color pattern of fluorescent barcodes that can be individually resolved and counted. Sample preparation was performed exactly per the manufacturer recommendations, and the raw data (.RCC files) quality control was conducted. Raw data was checked through the nSolver 4.0 software to ensure 1) binding density was appropriate, 2) ligation controls were in the appropriate range, and 3) positive hybridization controls were correct. These analyses were performed with nSolver™ 4.0 and exported raw data.

Datasets were normalized in nSolver™ by background thresholding the geometric mean across the negative controls, any samples outside of the 0.3 to 3 normalization factor range were omitted. Subsequently, normalization of the geometric mean of the positive controls was conducted to account for hybridization efficiency. CodeSet content is normalized to the geometric mean across 3 housekeeping genes (ABCF1, GUSB, HPRT1). Any samples for which the normalization factors were outside of the 0.1 to 10 range were omitted.

A heat map summary of the miRNA ratios was generated using Broad Institute's https://software.broadinstitute.org/morpheus/ Morpheus software.

Gene Expression RT-qPCR

Isolated total RNA from cell cultures samples were normalized to 500 ng of input for reverse transcription using oligo(dT) primers and cDNA synthesis using SuperScript IV (ThermoFisher, 18090010) according to the manufacturer's protocol. Each cDNA sample (5 µL) was added to MicroAmp Optical 96-well reaction plates (Invitrogen, ThermoFisher Applied Biosystems™, N8010560) containing 15 mL of Taqman Fast Advanced Master Mix (Invitrogen, ThermoFisher Applied Biosystems, 4444554). RT-qPCR was performed on Applied Biosystems QuantStudio 5 thermocycler with 1 cycle of 95℃ for 20 sec, followed by 40 cycles of 95℃ for 1 sec denaturation and 60℃ for 20 sec (annealing/extension). Specific NFQ-MGB TaqMan Advanced assay probes (ThermoFIsher PN4331348) were used for each gene present in the assay. $2^{\Delta\Delta Ct}$ calculations were performed and results were reported as ratios by normalizing the target gene to a housekeeping mRNA (GAPDH, ThermoFisher PN4448489), and each target gene to each probe for both negative siRNA and target siRNA.

miRNA RT-qPCR

Isolated RNA tissue samples were normalized to 10 ng of input for reverse transcription and cDNA synthesis using Taqman Advanced miRNA cDNA Synthesis Kit (Invitrogen, ThermoFisher Applied Biosystems™, A28007) according to the manufacturer's protocol. Each cDNA sample (5 µL) was added to MicroAmp Optical 96-well reaction plates (Invitrogen, ThermoFisher Applied Biosystems™, N8010560) containing 15 µL of Taqman Fast Advanced Master Mix (Invitrogen, ThermoFisher Applied Biosystems, 4444554). RT-qPCR was performed on Applied Biosystems QuantStudio 5 thermocycler with 1 cycle of 95℃ for 20 sec, followed by 40 cycles of 95℃ for 1 sec denaturation and 60℃ for 20 sec (annealing/extension). Specific NFQ-MGB TaqMan Advanced miRNA assay probes (Invitrogen, ThermoFisher Applied Biosystems, A25576) were used for each miRNA present in the assay. A miRNA standard curve was established using a universal standard curve with a non-mammalian exogenous 5' phosphorylated standard, Arabidopsis thaliana miRNA ath-159a (Invitrogen, ThermoFisher, 478411_mir). miRNA copy numbers were calculated using the synthetic miR ath-159a, utilizing the similarity of short miRNA sequences to amplify at the same rate (within 0.5 cycle threshold) with no cross-specificity between synthetic and human miRNA. A dynamic range of 10,000,000 to 100 copies was established and verified with synthesized human miRNA standards to validate ath-159a as a universal miRNA standard curve. Final copy number per 10 ng RNA was quantified and normalized to determine fold change expression over the negative mimic control.

Mouse Tissue RNA Extraction

Whole brain mouse tissues were sourced from Brain Bits LLC (Springfield, IL). Samples were flash frozen immediately after resection from C57BL/6 6 mice. Additional tissue samples were obtained from Charles River Laboratories (Wilmington, MA). Twenty milligram sections were cut by scalpel and placed in a 1.5 mL Eppendorf tube and stored at -80℃.

For RNA isolation, each tissue sample was thawed on ice. Qiazol (Qiagen) and chloroform were chilled on ice prior to use. Qiazol (700 µL) was added to each tube containing a tissue section, and disposable RNase-free pestles were used to homogenize the tissue. Subsequently, 140 µL of chloroform was added and centrifuged at maximum speed for 10 min. The upper aqueous phase (300 µL) was transferred to a new tube and 450 µL of 100% ethanol at room temperature was then added and mixed. Approximately 700 µL of this mixture was transferred to a Qiagen miRneasy column. The remaining steps in this process was performed according to the manufacturer's protocol (Qiagen miRneasy Kit, 217004). Each RNA sample in this report was analyzed by a NanoDrop spectrophotometer (ThermoFisher Scientific, Wilmington, MA) to confirm sample quality as recommended by nCounter® miRNA Expression Assay User Manual.

nanoString Mouse miRNA Profiling

miRNA profiling using nanoString (NanoString Technologies Inc. Seattle, WA) was performed exactly as per the manufacturer protocol (nCounter® miRNA Expression Assay User Manual). Each total RNA sample was analyzed in a separate multiplexed reaction. Briefly, unique oligonucleotide tags are ligated onto miRNAs, allowing short RNAs to be detected without amplification. Multiplexed hybridization of specific tags to their target miRNA, a biotin capture probe, and a unique reporter probe form a Target-Probe complex were hybridized in solution. After hybridization, the hybridization mixture containing the target/probe complexes is allowed to bind to magnetic beads complementary to sequences on the capture probe. Wash steps ensure excess probes without a complementary target were removed using a two-step magnetic bead-based purification. Final purified target/probe complexes are eluted off the beads, immobilized, and aligned to the cartridge. Barcodes were read on a digital analyzer in a high-throughput automated fashion for up to 600 individual miRNAs per sample. Quantification was performed on a nanoString SPRINT instrument with the nanoString Mouse miRNA Panel 1.5.

All individual tissue samples were analyzed with the mouse miRv1.5 panel on the nanoString Sprint instrument. Sample preparation was performed exactly per the manufacturer recommendations, and the raw data (.RCC files) quality control was conducted. Raw data was checked through the nSolver 4.0 software to ensure 1) binding density was appropriate, 2) ligation controls were in the appropriate range, and 3) positive hybridization controls were correct. These analyses were performed with nSolver™ 4.0 and exported raw data.

Datasets were normalized in nSolver™ by background thresholding the geometric mean across the negative controls, any samples outside of the 0.3 to 3 normalization factor range were omitted. Subsequently, normalization to the geometric mean of the positive controls was conducted to account for hybridization efficiency and was scaled to all endogenous and housekeeping genes to 1,000,000 total count of the lane. Any samples for which the

normalization factors were outside of the 0.1 to 10 range were omitted. A heat map summary of the miRNA ratios was generated using Broad Institute's https://software.broadinstitute.org/morpheus/ Morpheus software.

In silico generation of miR-T cassettes

A computer script written in the Python programming language was written to generate miR-T cassettes that are optimal for RISC targeting. This script inserts the correct target sequence in the cassette such that no two targets are repeated in-line, to prevent potential steric occlusion of RISC occupied adjacent targets. It also searches for tumor specific miRNA targets or seed targets that may be present by chance as random spacers are generated. If these sequences are encountered, these candidates are eliminated. Then an automated effort to eliminate structured elements is performed, as RNA secondary structure is also a known inhibitor of RISC targeting (Ameres et al. 2007). The optimal lowest predicted structured cassette is then selected. These cassettes were then validated individually with a well validated tool to detect miRNA binding sites objectively called miRANDA.

Biodistribution Studies

BALB/c mice bearing established (~100 mm^3) dual flank A20 tumors were administered $3x10^5$-$3x10^6$ PFU, depending upon the study of ONCR-159 into the right flank tumor. Tissues (injected and contralateral tumors, liver, and blood) were harvested 4, 24, 48, 72, and 168 hours post dose. Genomic viral DNA from tumors and liver was quantified using the nanodrop and diluted to 25 ng/µl in nuclease free water. Blood samples were diluted to 10 ng/µl. Five µl/well of either the DNA sample (corresponding to 125 ng of DNA from tumors or 50 ng of DNA from blood) or the US6 plasmid standard was used in a qPCR reaction, performed in technical triplicates, to detect HSV-1 genomes on a Quantstudio5 qPCR instrument with the following thermal cycler conditions: Hold Stage: 95˚C for 1 second, PCR stage: 95^{o}C for 1 second, followed by 60˚C for 30 seconds. The PCR stage was performed for 45 cycles. The plasmid standards used in the assay were used to generate a standard curve with known amount of copies corresponding to a set of Ct values. Based on this standard curve, the amount of HSV genome copies in the sample were calculated. The copy number calculations were done on the Quantstudio software. Since 125 ng/well of tumor DNA or 50 ng/well of blood DNA was loaded in the qPCR assay, a conversion factor was applied to the copy number in order to plot them as copies/µg of DNA. Technical duplicates were averaged and the results of individual animals within each group were plotted using GraphPad software. Conversion of copy number to copies/µg and calculations of averages were done on Microsoft Excel. PCR Primer/probe: Fwd: 5'-CCCGCTGGAACTACTATGACA-3'; Rev: 5'-GCATCAGGAACCCCAGGTT-3'; Probe: 5'-TTCAGCGCCGTCAGCGAGGA-3' with FAM as the reporter dye and MGB-NFQ as the quencher.

TABLES

Table S1. siRNA sequences utilized in the siRNA screen

Target Gene	siRNA sequence
ICP0 siRNA 1	GGGAGGGAGACAAGAGGAA
ICP0 siRNA 2	CCACCACGGACGAGGAUGA
ICP0 siRNA 3	GGACGAGGGAAAACAAUAA
RS1-ICP4 siRNA 1	ACGAGGACGACGACGGCAA
RS1-ICP4 siRNA 2	CCGCGGACCUGCUGUUUGA
RS1-ICP4 siRNA 3	CGGACUUCUGCGAGGAGGA
UL5 siRNA 1	CCAGCUAGACGGACAGAAA
UL5 siRNA 2	UCAUGAAGGUGCUGGAGUA
UL5 siRNA 3	GCUCAUAUUUAGCGGGCUU
UL8 siRNA 1	GCACGGGACUGGUGGUGAA
UL8 siRNA 2	GCUCAUCACCUGCGCGAAA
UL8 siRNA 3	CGACGGAGCUGCGGGAUUU
UL9 siRNA 1	CAACAAAUUCCGUUACAAA
UL9 siRNA 2	CAGUACACGUCGAGCGUAU
UL9 siRNA 3	CCAAUUACAUUAUGAACGA
UL29-ICP8 siRNA 1	ACUGCGACGUGCUGGGAAA
UL29-ICP8 siRNA 2	CCGACAAGCGCGUGGACAU
UL29-ICP8 siRNA 3	GCGAGGACAUCGAGACCAU
UL30 siRNA 1	CCAUCAAGGUCGUGUGUAA
UL30 siRNA 2	AGAAGAAGGACCUGAGCUA
UL30 siRNA 3	AGAUAAAGGUGAACGGCAU
UL39-40 siRNA 1	GGGAAAUGUUCAAGUUCUU
UL39-UL40 siRNA 2	GCAUAUAAGCGCGGACUAA
UL39-UL40 siRNA 3	GGGAGGAGUUCGAGAAGCU
UL42 siRNA 1	GGACACGGCCCUAAAGAAA
UL42 siRNA 2	GCGCCGAACUUAAUGGAAU
UL42 siRNA 3	CCGUUGAGCUAGCCAGCGA
UL48-VP16 siRNA 1	CAACAUGUCCAGAUCGAAAUU
UL48-VP16 siRNA 2	GGUACAGGGCCGAGCAGAAUU
UL48-VP16 siRNA 3	GCAAACAGCUCGUCGACCAUU
UL54-ICP27 siRNA 1	CGGACGAGGACAUGGAAGA
UL54-ICP27 siRNA 2	GCGCACAGGUCAUGCACGA
UL54-ICP27 siRNA 3	UGGCGGACAUUAAGGACAU
US1-ICP22 siRNA 1	GGAGUGUGAUCUUAGUAAU
US1-ICP22 siRNA 2	CGACAAGCGAUGAUGAAAU
US1-ICP22 siRNA 3	ACUGUUACCUGAUGGGAUA

siRNA, small interfering RNA.

Table S2. Total number of normal and malignant human tissues assessed

Tissue	Normal	Malignant
Skin	4	14
Head & Neck	10	10
Lung	20	18
Breast	0	10
Liver	8	4
Pancreas	11	10
Colon	5	12
Bladder	18	7
Ovary	0	19
Brain	10	0
Heart	6	0
Spinal Cord	4	0
Nerve	4	0
Artery	3	0
Vein	6	0
Ganglion	1	0
Total	110	104

Table S3. Summary of the normal tissue specimens used in this study

Normal Tissue (Total)	**Subtype(s) (Total)**
Skin (4)	Skin structure (3), Skin and subcutaneous tissue (1)
Head & Neck (10)	Oral Cavity: Tongue (5), Larynx (1), Esophagus (1) Oropharynx (3)
Lung (20)	Lung normal adjacent uninvolved (20)
Liver (8)	Liver normal adjacent uninvolved (8)
Pancreas (11)	Pancreatic body, normal adjacent uninvolved (11)
Colon (5)	Colon normal adjacent uninvolved (5)
Bladder (18)	Bladder normal adjacent uninvolved (18)
Brain (10)	Temporal lobe (3), Parietal lobe (1), Normal brain (6)
Heart (6)	Heart normal adjacent uninvolved (6)
Spinal Cord (4)	Spine normal adjacent uninvolved (4)
Nerve (4)	Nerve normal adjacent uninvolved (4)
Artery (3)	Artery normal adjacent uninvolved (3)
Vein (6)	Vein normal adjacent uninvolved (6)

Table S4. Summary of the malignant tissue specimens used in this study

Malignant Tissue (Total)	Subtype(s) (Total)
Skin (14)	Primary melanoma (4), Melanoma metastases (9), Uveal melanoma (1)
Head & Neck (10)	Nasopharynx (1), Tongue (1), Squamous cell carcinoma: Larynx (1), Oropharynx (1), Tongue (5), Soft palate (1)
Lung (18)	Carcinoma: Bronchioalveolar (1), Non-small cell (2), Adenocarcinoma (5), Squamous cell (6), Adenoid cystic (1), Mucosa-associated lymphoma (1), Adenosquamous (2)
Breast (10)	Carcinoma: Infiltrating ductal (5), Triple negative (5)
Liver (4)	Carcinoma: Hepatocelluar (1), Neuroendocrine (1), Adenocarcinoma (1), Invasive ductal (1)
Pancreas (10)	Ductal Adenocarcinoma (7), Neuroendocrine (1), Endocrine (1), Metastatic liver carcinoma (1)
Colon (12)	Adenocarcinoma (12)
Bladder (7)	Urothelial carcinoma (6) Squamous cell (1)
Ovary (19)	Carcinoma (17), Sarcoma (2)

Table S5. Mouse homology and seed conservation with human mature miRNA

miRNA	Species	Mature miRNA sequence	Homology
miR-124-3p	Human	uaaggcacgcggugaaugccaa	100%
	Mouse	uaaggcacgcggugaaugcc	100%
miR-1-3p	Human	uggaauguaaagaaguauguau	100%
	Mouse	uggaauguaaagaaguauguau	100%
miR-143-3p	Human	ugagaugaagcacuguagcuc	100%
	Mouse	ugagaugaagcacuguagcuc	100%
miR-128-3p	Human	ucacagugaaccggucucuuu	100%
	Mouse	ucacagugaaccggucucuuu	100%
miR-137-3p	Human	uuauugcuuaagaauacgcguag	100%
	Mouse	uuauugcuuaagaauacgcguag	100%
miR-122-5p	Human	uggagugugacaaugguguuug	100%
	Mouse	uggagugugacaaugguguuug	100%
miR-219a-1-5p	Human	ugauuguccaaacgcaauucu	100%
	Mouse	ugauuguccaaacgcaauucu	100%
miR-126-3p	Human	ucguaccgugaguaauaaugcg	100%
	Mouse	ucguaccgugaguaauaaugcg	100%
miR-204-5p	Human	uucccuuugucauccuaugccu	100%
	Mouse	uucccuuugucauccuaugccu	100%
miR-217-5p	Human	uacugcaucaggaacugauugga	100%
	Mouse	uacugcaucaggaacugacugga	100%

Table S6. miRNA mimics used in this study

miRNA	miRNA ID	Mature miRNA Sequence[1]	miRBase Accession #	miRvana miRNA mimic Assay ID[2]	ThermoFisher Lot #
Neg	**Neg[3]**	SCRAMBLED	NA		
hsa-mir-124-3p	**124**	UAAGGCACGCGGUGAAUGCCAA	MIMAT0000422	MC10060	ASO2B3UW
hsa-mir-1-3p	**1**	UGGAAUGUAAAGAAGUAUGUAU	MIMAT0000416	MC10617	ASO28P3N
hsa-mir-143-3p	**143**	UGAGAUGAAGCACUGUAGCUC	MIMAT0000435	MC10883	ASO28P30
hsa-mir-128-3p	**128**	UCACAGUGAACCGGUCUCUUU	MIMAT0000424	MC11746	ASO28P3M
hsa-mir-219a-5p	**219a**	UGAUUGUCCAAACGCAAUUCU	MIMAT0000276	MC10664	ASO28W92
hsa-mir-122-5p	**122**	UGGAGUGUGACAAUGGUGUUUG	MIMAT0000421	MC11012	ASO28ASS
hsa-mir-137-3p	**137**	UUAUUGCUUAAGAAUACGCGUAG	MIMAT0000429	MC10513	ASO29BRX
hsa-mir-217-5p	**217**	UACUGCAUCAGGAACUGAUUGGA	MIMAT0000274	MC12774	ASO2AYTD
hsa-mir-126-3p	**126**	UCGUACCGUGAGUAAUAAUGCG	MIMAT0000445	MC12841	ASO28W50

miRNA, microRNA; NA, not applicable; Neg, negative.

[1]Mature miRNA resulting from Drosha and Dicer processing, the sequence as defined by miRbase is shown here.

[2]miRvana miRNA mimics are mature miRNA (20-22 nucleotides long), chemically modified, double stranded RNA molecules designed to bind and mimic endogenous miRNA molecules.

[3]The negative control for cognate miRNA mimic assays (Neg mimic) is a scrambled, non-targeting sequence.

Table S7: miRNA in-situ hybridization citations for miRNAs included in ONCR-159

miRNA	Cellular/Tissue expression	Reported Function	Reference
hsa-miR-1-3p	Skeletal / Cardiac Muscle	Promotes myoblast differentiation, known and to suppress tumor growth.	[3, 4]
hsa-miR-122-5p	Liver	Most abundant liver miRNA, tumor suppressor.	[5, 6]
hsa-miR-124-3p	CNS / Neurons	Neuron specific. Inhibits cellular proliferation.	[7, 8]
hsa-miR-126-3p	Endothelium	Required for endothelial development and healing. Downregulated in tumors.	[9-11]
hsa-miR-128-3p	CNS / Neurons	Important for neural development. Reported use for neuron miR-T development.	[12, 13]
hsa-miR-137-3p	CNS / Neurons	Enriched in neurons, important for neural development.	[14]
hsa-miR-143-3p	Smooth Muscle	Enriched in muscle, tumor suppressor.	[15, 16]
hsa-miR-204-5p	Brain	Loss associated with glioma progression.	[17]
hsa-miR-217-5p	Pancreas, other	Downregulates MALAT1, the miRNA-216 (contains miR-217) cluster is considered a tumor suppressor cluster.	[18-20]
hsa-miR-219a-5p	Brain, oligodendrocytes	Important for oligodendrocyte differentiation and myelination. Depleted in hepatocellular carcinoma tissue and glioblastoma, potential tumor suppressive effects.	[21-23]

FIGURES

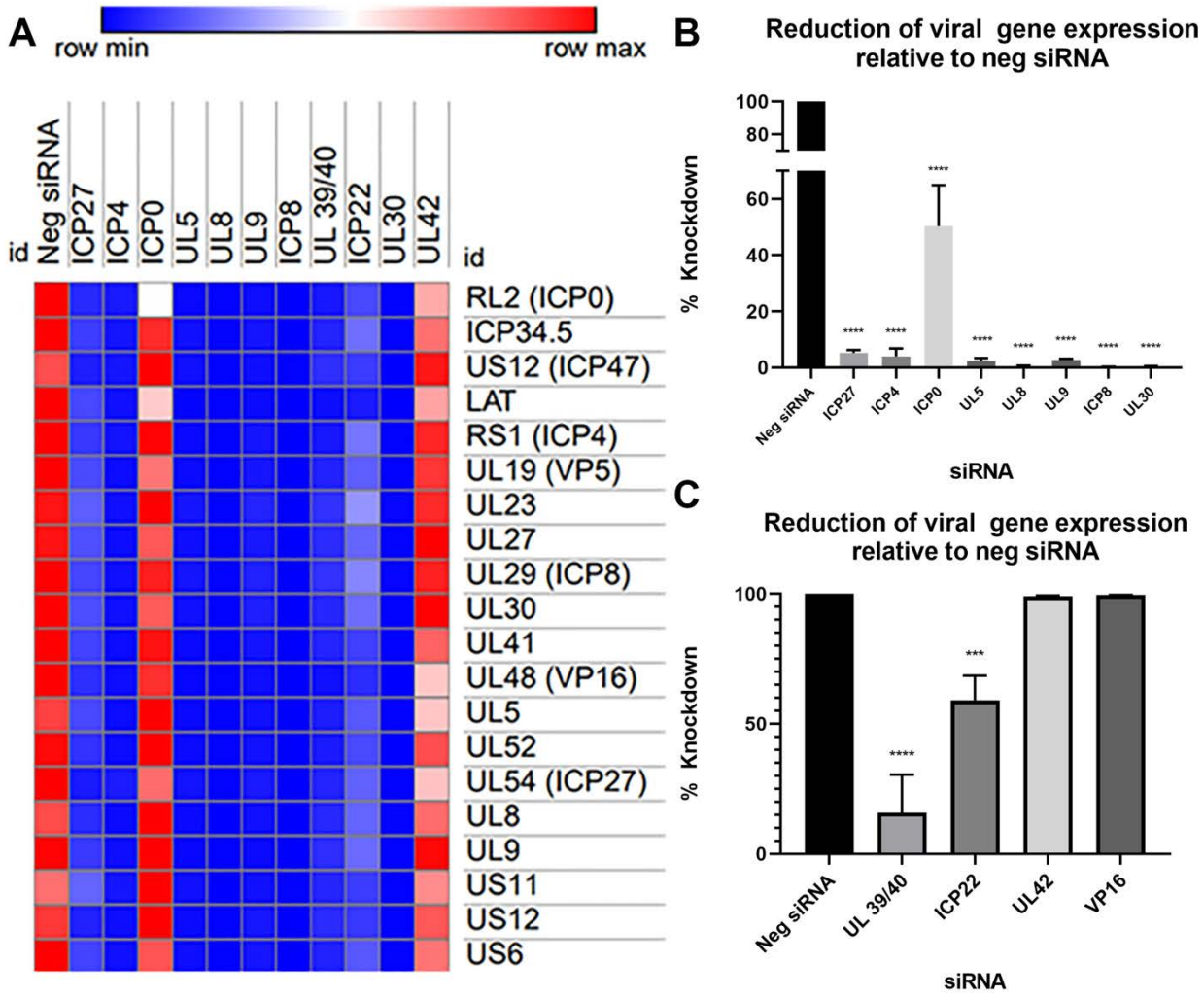

Figure S1. Efficiency of siRNA pool mediated HSV-1 transcript repression. Both nanoString TagSet and RT-qPCR were utilized to assess transcriptional knockdown achieved by pooled siRNA for each target HSV-1 gene. **(A)** Heatmap expression levels comparing target siRNA to negative siRNA using a custom nanoString TagSet consisting of 20 HSV-1 genes. **(B)** nanoString TagSet comparison of gene expression as a percentage (%) of negative siRNA. **(C)** 4 target genes not included in the nanoString TagSet were evaluated by ΔΔ RT-qPCR and plotted as a percentage (%) of negative siRNA. One-way ANOVA Dunnett's multiple comparisons test was used for statistical analysis. ***p<0.005; ****p<0.0001.

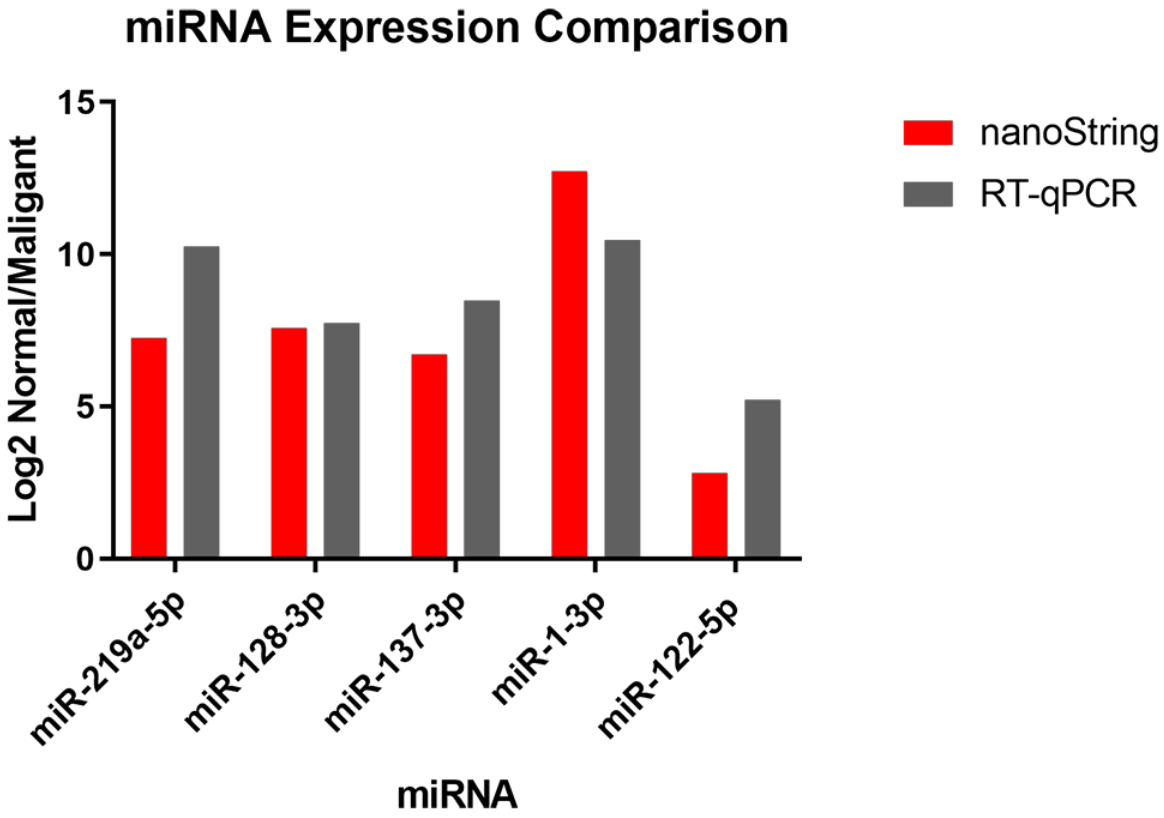

Figure S2. Comparison of miRNA Fold Change Expression by nanoString vs. miRNA RT-qPCR. miRNA RT-qPCR was performed in technical triplicate to quantify miRNA expressed in endogenous tissue from 5 normal human brain, 5 heart, 4 liver, 5 malignant lung, and 4 malignant liver tissue isolates. For each bar shown in the figure, normal tissue fold change/malignant between miRNA copy number and nanoString miRNA counts are compared. Values are plotted in Log2 to compare significantly different readouts. miRNA, microRNA; RT-qPCR, reverse transcriptase quantitative polymerase chain reaction.

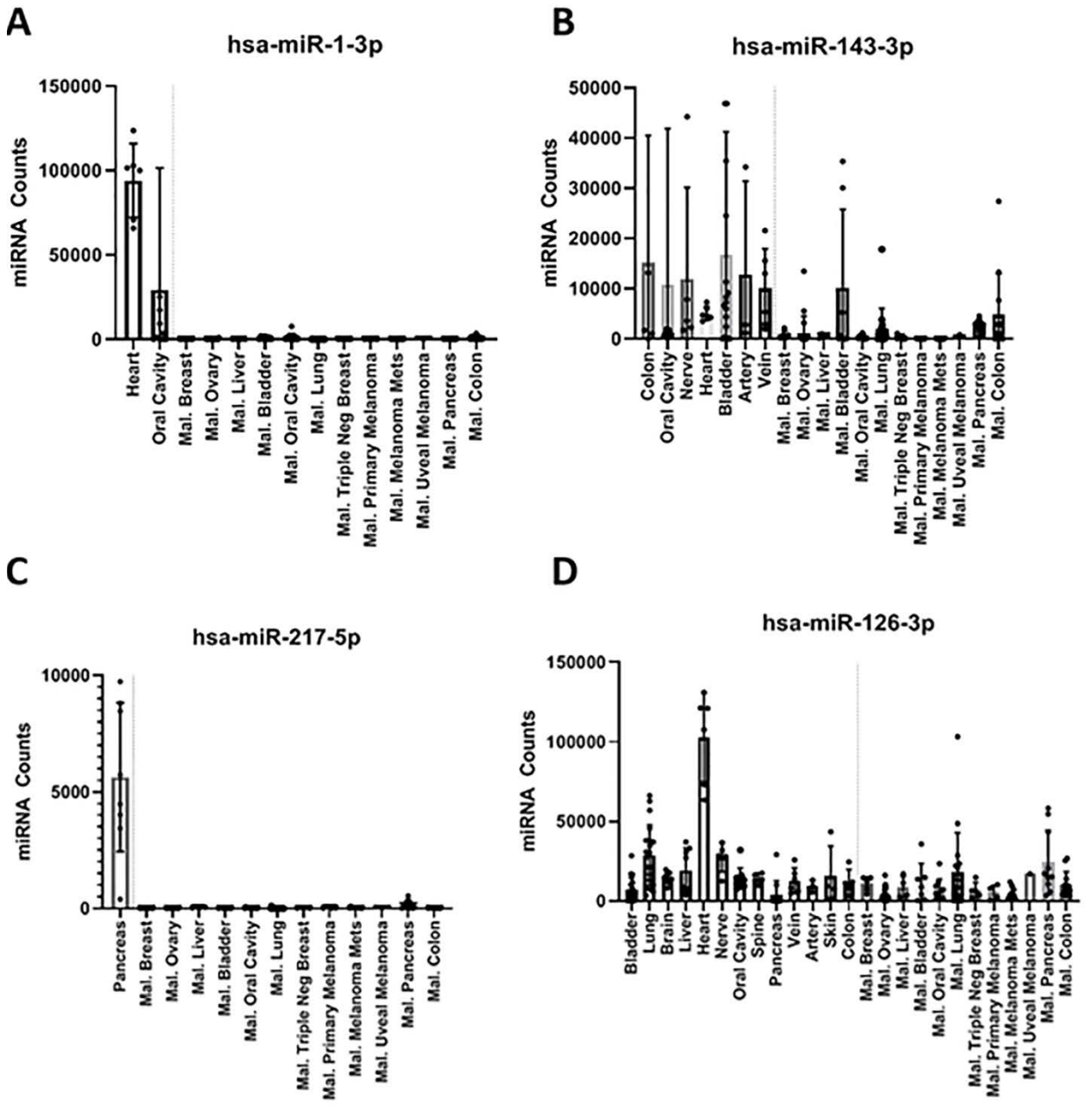

Figure S3. Global Expression Profiling of Human Normal and Malignant Tissue miRNAs to Identify miRNAs for Host Tissue Protection. Individual nanoString miRNA counts of multiple tissues of interest for additional host tissue protection are compared to each malignant tissue profiled. Highly-expressed normal tissue miRNAs are shown for cardiac and smooth muscle **(A & B)**, pancreas **(C)**, and endothelium **(D)**. Mal, malignant.

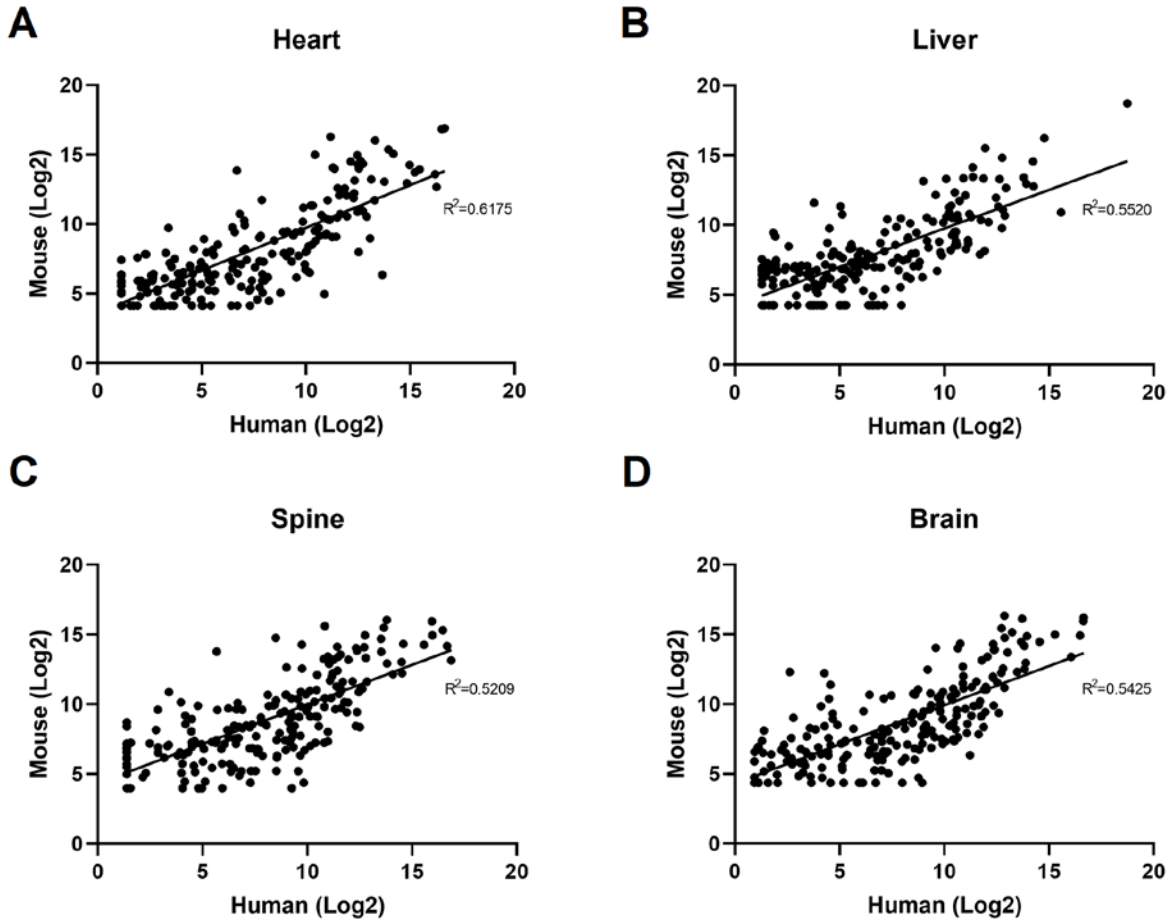

Figure S4. Comparison of Expression Levels of miRNA in Human and Murine Tissues. Individual miRNA counts of multiple tissue types were compared between species for individual miRNA expression. 216 miRNA (100% conserved mature miRNA sequence overlap between both human and mouse miRNA nanoString panels) counts are plotted in Log2 scale. Mouse miRNA are plotted on the Y-axis and human miRNA are plotted on the X-axis. Each graph is fit by a linear regression curve. In panels **A**-**D**, 6 heart, 8 liver, 4 spine and 10 brain human tissues are compared to 3 mouse tissue samples of each tissue type. Linear regression (Goodness of fit test) was calculated with GraphPad Prism (8.0).

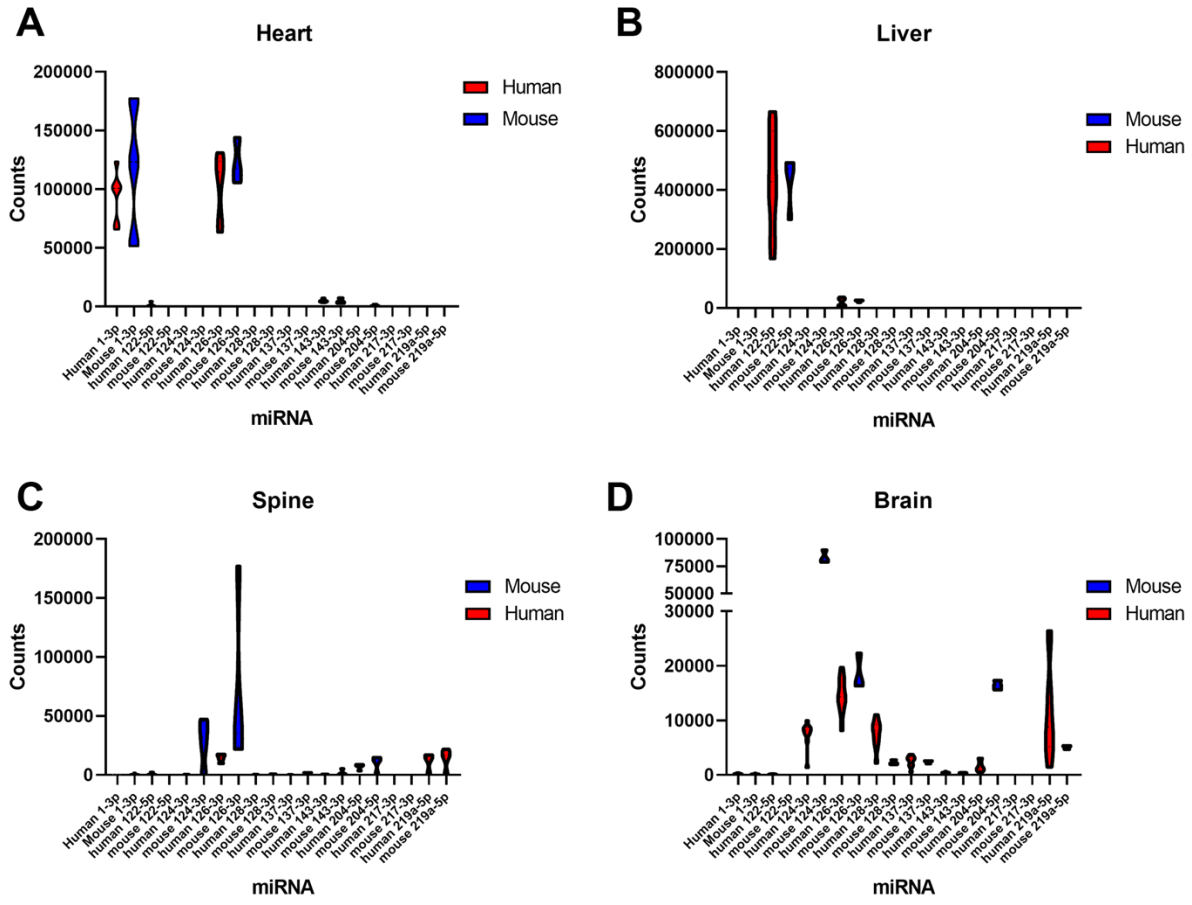

Figure S5. Comparison of miRNA Level of Expression in a Subset of miRNA. Individual miRNA counts of multiple tissue types were compared between species for multiple miRNAs that comprise the ONCR-159 miR-T configuration. In panels **A**-**D**, 6 heart, 8 liver, 4 spine and 10 brain human tissues are compared to 3 mouse tissue samples of each tissue type.

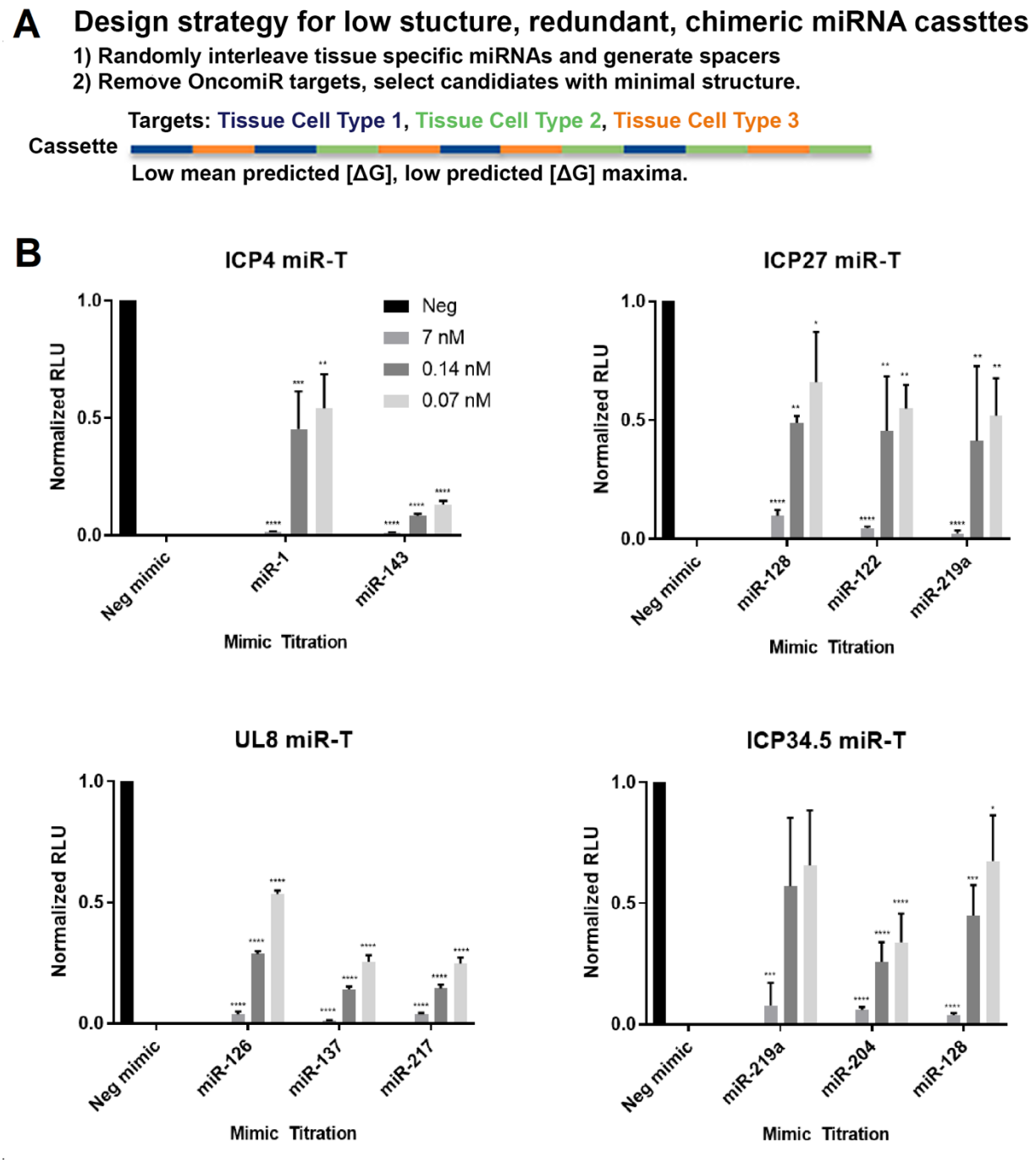

Figure S6. Next-generation of Minimal Size and Maximize Efficacy of miR-T Cassettes. (A) Description of the bioinformatics processes for miR-T cassette designs. Briefly, cassettes were made *in silico* and were scanned to reduce secondary structure and spurious miRNA targeting. **(B-E)** Dual-luciferase constructs were constructed with psiCHECK™-2 and tested in a mimic titration to validate efficient repression *in vitro* for the cassettes included in the ICP4, ICP27, UL8, and ICP34.5 loci, respectively. miRvana miRNA mimic titrations were co-transfected in HEK293 cells using Lipofectamine 2000 and 50 ng of plasmid DNA for the vector containing the miR-T in biological and technical triplicate. miRNA, microRNA; miR-T, miRNA-binding cassettes; Neg, negative. One-way ANOVA Dunnett's multiple comparisons test was used for statistical analysis. *p<0.05; **p<0.01; ***p<0.005; ****p<0.0001.

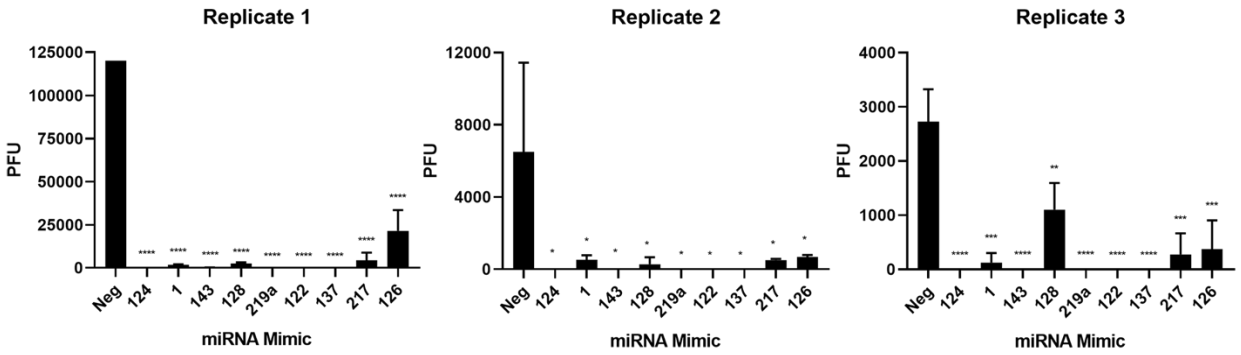

Figure S7. Individual miRNA Attenuates ONCR-159 Viral Replication. Viral replication was assessed in A253 cells transfected with the indicated mimics and infected with ONCR-159 for 72 hrs. Viral replication is shown as total PFU counts determined by virus plaque titer assay. PFU is plotted across 3 individual replicas. Statistical significance was calculated using Bonferroni-Dunn Student's T-test, *p<0.05; **p<0.01; ****p<0.005; **** p<0.00001. PFU, plaque forming units. miRNA, microRNA; miR-T, Neg, negative; PFU, plaque-forming unit.

Figure S8. Physiologic Validation of Mimic Amounts Used in miRNA Mimic Assay. A253 cells transiently transfected with miRNA mimics were collected for RNA isolation at 24 hours post-transfection. This parallels the time point at which viral infection is performed for viral replication assessment. miRNA RT-qPCR was performed in technical triplicate to quantify transient miRNA expressed *in vitro* in relation to endogenous miRNA levels from 5 human brain tissue isolates. Fold change (FC) was determined by normalizing miRNA copy number from cells transiently transfected miRNA mimics to miRNA levels expressed in human brain normal tissue. Assessment of levels of expression of **(A)** hsa-miR-124-3p, **(B)** hsa-miR-128-3p, and **(C)** hsa-miR-137-3p. Supernatant from A253 cells transiently transfected with mimic miRNA and infected with ONCR-159 at 0.1 multiplicity of infection were collected after 3 days. Viral production was determined in a plaque assay in Vero cells. (**D)** Three miRNA endogenously expressed in human brain tissue, hsa-miR-124-3p, hsa-miR-128-3p, and hsa-miR-137-3p, were titrated to define a dynamic threshold to assess miRNA-mediated viral replication of ONCR-159. Titer ratio was determined by normalizing the plaque counts obtained by the negative mimic control. Statistical significance was calculated using Bonferroni-Dunn student's T-test, ****$p<0.00001$; **$p=0.003$. FC, fold change; miRNA, microRNA; Neg, negative; RT-qPCR, reverse transcriptase quantitative polymerase chain reaction.

Figure S9. **ONCR-159 Viral Biodistribution Kinetics in the A20 Syngeneic Bilateral Tumor Model.** Viral genomic (US6/gD locus) DNA levels were quantified within the indicated tissues by a qRT-PCR assay either (**A)** 24 hours after a $3x10^5$ PFU IT dose or (**B)** at the indicated time point after a $3x10^6$ PFU IT dose of ONCR-159. The sensitivity limit of the assay (40 genome copies/µg DNA) is indicated as a dashed line. **(A)** N=5/group; **(B)** N=7/group.

Figure S10. Efficacy of ONCR-157 and ONCR-159 on the A20, MC38, and B16F10N1 Tumor Models. Individual tumor volume curves for each treatment are shown after IT administration of PBS or $3x10^6$ PFU (A20; MC38) or $6x10^6$ (B16F10N1) PFU of ONCR-159 or ONCR-157. Dosing occurred on days 1, 4, and 7, where Day 1 = day of dose initiation. N=8-10 mice/group.

References

1. Ameres, SL, Martinez, J, and Schroeder, R (2007). Molecular basis for target RNA recognition and cleavage by human RISC. *Cell* **130**: 101-112.
2. Enright, AJ, John, B, Gaul, U, Tuschl, T, Sander, C, and Marks, DS (2003). MicroRNA targets in Drosophila. *Genome Biol* **5**: R1.
3. Gagan, J, Dey, BK, Layer, R, Yan, Z, and Dutta, A (2012). Notch3 and Mef2c proteins are mutually antagonistic via Mkp1 protein and miR-1/206 microRNAs in differentiating myoblasts. *J Biol Chem* **287**: 40360-40370.
4. Xie, D, Song, H, Wu, T, Li, D, Hua, K, Xu, H, *et al.* (2018). MicroRNA424 serves an antioncogenic role by targeting cyclindependent kinase 1 in breast cancer cells. *Oncol Rep* **40**: 3416-3426.
5. Fornari, F, Gramantieri, L, Giovannini, C, Veronese, A, Ferracin, M, Sabbioni, S, *et al.* (2009). MiR-122/cyclin G1 interaction modulates p53 activity and affects doxorubicin sensitivity of human hepatocarcinoma cells. *Cancer Res* **69**: 5761-5767.
6. Gramantieri, L, Ferracin, M, Fornari, F, Veronese, A, Sabbioni, S, Liu, CG, *et al.* (2007). Cyclin G1 is a target of miR-122a, a microRNA frequently down-regulated in human hepatocellular carcinoma. *Cancer Res* **67**: 6092-6099.
7. Cheng, LC, Pastrana, E, Tavazoie, M, and Doetsch, F (2009). miR-124 regulates adult neurogenesis in the subventricular zone stem cell niche. *Nat Neurosci* **12**: 399-408.
8. Silber, J, Hashizume, R, Felix, T, Hariono, S, Yu, M, Berger, MS, *et al.* (2013). Expression of miR-124 inhibits growth of medulloblastoma cells. *Neuro Oncol* **15**: 83-90.
9. Fish, JE, Santoro, MM, Morton, SU, Yu, S, Yeh, RF, Wythe, JD, *et al.* (2008). miR-126 regulates angiogenic signaling and vascular integrity. *Dev Cell* **15**: 272-284.
10. Hamada, S, Satoh, K, Fujibuchi, W, Hirota, M, Kanno, A, Unno, J, *et al.* (2012). MiR-126 acts as a tumor suppressor in pancreatic cancer cells via the regulation of ADAM9. *Mol Cancer Res* **10**: 3-10.
11. Jusufovic, E, Rijavec, M, Keser, D, Korosec, P, Sodja, E, Iljazovic, E, *et al.* (2012). let-7b and miR-126 are down-regulated in tumor tissue and correlate with microvessel density and survival outcomes in non--small--cell lung cancer. *PLoS One* **7**: e45577.
12. Smirnova, L, Grafe, A, Seiler, A, Schumacher, S, Nitsch, R, and Wulczyn, FG (2005). Regulation of miRNA expression during neural cell specification. *Eur J Neurosci* **21**: 1469-1477.
13. Skalsky, RL, and Cullen, BR (2011). Reduced expression of brain-enriched microRNAs in glioblastomas permits targeted regulation of a cell death gene. *PLoS One* **6**: e24248.
14. Smrt, RD, Szulwach, KE, Pfeiffer, RL, Li, X, Guo, W, Pathania, M, *et al.* (2010). MicroRNA miR-137 regulates neuronal maturation by targeting ubiquitin ligase mind bomb-1. *Stem Cells* **28**: 1060-1070.
15. Elia, L, Quintavalle, M, Zhang, J, Contu, R, Cossu, L, Latronico, MV, *et al.* (2009). The knockout of miR-143 and -145 alters smooth muscle cell maintenance and vascular homeostasis in mice: correlates with human disease. *Cell Death Differ* **16**: 1590-1598.
16. Kent, OA, McCall, MN, Cornish, TC, and Halushka, MK (2014). Lessons from miR-143/145: the importance of cell-type localization of miRNAs. *Nucleic Acids Res* **42**: 7528-7538.
17. Ying, Z, Li, Y, Wu, J, Zhu, X, Yang, Y, Tian, H, *et al.* (2013). Loss of miR-204 expression enhances glioma migration and stem cell-like phenotype. *Cancer Res* **73**: 990-999.
18. Zhao, WG, Yu, SN, Lu, ZH, Ma, YH, Gu, YM, and Chen, J (2010). The miR-217 microRNA functions as a potential tumor suppressor in pancreatic ductal adenocarcinoma by targeting KRAS. *Carcinogenesis* **31**: 1726-1733.
19. Wang, H, Dong, X, Gu, X, Qin, R, Jia, H, and Gao, J (2015). The MicroRNA-217 Functions as a Potential Tumor Suppressor in Gastric Cancer by Targeting GPC5. *PLoS One* **10**: e0125474.
20. Zhang, M, Li, M, Li, N, Zhang, Z, Liu, N, Han, X, *et al.* (2017). miR-217 suppresses proliferation, migration, and invasion promoting apoptosis via targeting MTDH in hepatocellular carcinoma. *Oncol Rep* **37**: 1772-1778.
21. Dugas, JC, and Notterpek, L (2011). MicroRNAs in oligodendrocyte and Schwann cell differentiation. *Dev Neurosci* **33**: 14-20.
22. Huang, N, Lin, J, Ruan, J, Su, N, Qing, R, Liu, F, *et al.* (2012). MiR-219-5p inhibits hepatocellular carcinoma cell proliferation by targeting glypican-3. *FEBS Lett* **586**: 884-891.
23. Rao, SA, Arimappamagan, A, Pandey, P, Santosh, V, Hegde, AS, Chandramouli, BA, *et al.* (2013). miR-219-5p inhibits receptor tyrosine kinase pathway by targeting EGFR in glioblastoma. *PLoS One* **8**: e63164.